Nanotechnology **23** (2012) 365701 (4pp) doi:10.1088/0957-4484/23/36/365701

Thermal conductivity measurements of suspended graphene with and without wrinkles by micro-Raman mapping

Shanshan Chen[1,2], Qiongyu Li[1], Qimin Zhang[1], Yan Qu[3], Hengxing Ji[2], Rodney S Ruoff[2] and Weiwei Cai[1]

[1] Department of Physics, Xiamen University, Xiamen 361005, People's Republic of China
[2] Department of Mechanical Engineering and the Materials Science and Engineering Program, The University of Texas, Austin, TX 78712, USA
[3] The Sixth Element (Changzhou) Materials Technology Co., Ltd, Changzhou, People's Republic of China

E-mail: r.ruoff@mail.utexas.edu and wwcai@xmu.edu.cn

Received 1 June 2012, in final form 9 July 2012
Published 21 August 2012
Online at stacks.iop.org/Nano/23/365701

Abstract
The thermal conductivity (κ) of suspended graphene membranes made by chemical vapor deposition (CVD) was measured by micro-Raman mapping. Cracks and wrinkles present in these suspended graphene membranes were identified by micro-Raman mapping, and κ values and their statistics were obtained on membranes free of such imperfections in a single mapping. Based on this new technique, an average κ value of 1875 ± 220 W m^{-1} K^{-1} at 420 K was measured on 26 suspended graphene membranes that were free of wrinkles, ~27% higher than the average value measured from 12 graphene membranes with wrinkles. These results suggest that the variation in published thermal conductivity values for suspended graphene samples could, at least in part, be due to the presence or absence of wrinkles.

(Some figures may appear in colour only in the online journal)

1. Introduction

The thermal transport of graphene, which has an extremely high thermal conductivity when suspended [1], is of fundamental and practical interest. Based on the dependence of the Raman G or 2D peak frequency on the temperature of suspended graphene heated by a Raman laser, there have been a number of recent studies exploring phonon transport by the non-contact optical method based on micro-Raman spectroscopy [2–7]. A thermal conductivity value of about 5000 W m^{-1} K^{-1} near room temperature was reported for a ~3 μm-long suspended monolayer graphene sample obtained by micromechanical exfoliation of highly oriented pyrolytic graphite (HOPG) [2]. However, it was suggested in our recent work that the ultrahigh thermal conductivity values reported earlier [2] were perhaps a result of the significantly overestimated optical absorption used for such samples [8] as we found that the thermal conductivity of a ~3.8 μm suspended CVD-grown graphene is about 2500 W m^{-1} K^{-1} near room temperature by measuring the optical absorption coefficient, and also by subtracting the thermal contact resistance [3] and also the heat loss to air [4]. The thermal conductivity of a ~44 μm diameter suspended graphene monolayer was reported as about 600 W m^{-1} K^{-1} when the center was heated by laser excitation to a temperature of about 660 K, with the temperature measured from the anti-Stokes to Stokes ratio of the Raman scattering signals [6]. More recently, Lee *et al* reported their measurements of the thermal conductivity of suspended graphene using the same non-contact optical method on a sample obtained by micromechanical exfoliation from natural graphite flakes [7]; they obtained values ranging from ~1800 W m^{-1} K^{-1} near room temperature to ~710 W m^{-1} K^{-1} near 500 K. They assumed a value for the absorption of the laser power based on a reported absorption of 2.3% of light [8], and thus did not

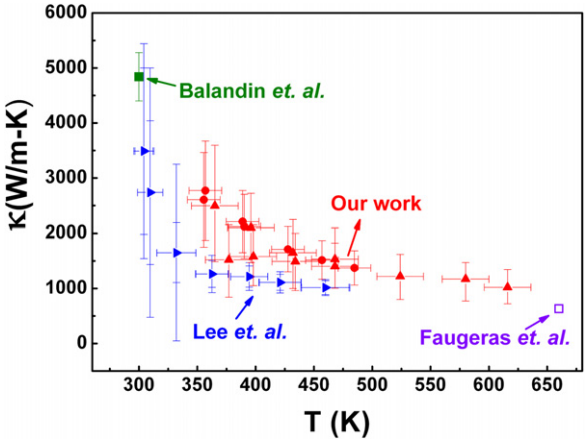

Figure 1. Thermal conductivity values of suspended graphene from recently published papers [2, 4, 6, 7]. Reprinted with permission from [7]. Copyright 2011 by the American Physical Society.

measure the absorbed power directly during the non-contact measurement.

Figure 1 shows experimental data for the thermal conductivity κ in suspended graphene from recently published papers, with reported values varying from ~1500 to 5000 W m^{-1} K^{-1} near room temperature [2, 4, 6, 7]. Perhaps the large variation in thermal conductivity values could also be attributed, in part, to differences in the presence of small defects such as cracks or wrinkles from sample to sample. However, most of the thermal conductivity values so far have been extracted from measurements on a single sample, which suggests that it is important to obtain κ values and their statistics over many graphene membranes. In this paper, we report an improved non-contact micro-Raman mapping technique to measure the thermal conductivity of suspended graphene and thus measurements on 38 membranes, of which 26 were wrinkle-free graphene membranes and 12 were graphene membranes with wrinkles.

2. Experimental methods

Graphene was grown on 25 μm thick Cu foils (Alfa Aesar, item No. 13382) on the inside surface of an 'enclosure' by CVD in a tube furnace with a methane flow rate of 1 sccm and a partial pressure of 36 mTorr at 1035 °C [9]. The graphene-on-Cu sample was spin coated with poly-methyl methacrylate (PMMA) that was then cured [10]. After the Cu substrate was dissolved in an $(NH_4)_2S_2O_8$ solution (0.3 M), the PMMA–graphene was lifted from the solution and transferred onto a Au-coated surface of a 200 nm thick, 0.5 × 0.5 mm^2, low-stress silicon nitride (SiN_x) membrane supported on a circular 3 × 3 mm^2 silicon frame [3, 4, 11]. The SiN_x membrane consisted of a 100 × 100 square array of 2.8 μm diameter holes at a pitch of 2.5 μm between holes. After transfer, the PMMA–graphene was dried in vacuum (10^{-1} Torr) for 1 h. Then, the PMMA was removed with acetone.

Figure 2(a) shows a scanning electron microscope (SEM, FEI Quanta-600) image of the monolayer graphene on the SiN_x holey membrane. Before the thermal transport measurement, micro-Raman (WITec Alpha-300) mapping was used to determine the local quality (e.g., defect density, cracks and wrinkles) and the number of (stacked) layers of the graphene films. As an example, figure 2(b) shows a typical 30 × 30 μm^2 integrated intensity Raman map of the 2D peak of the suspended graphene on a selected area. Arrows in the map show wrinkles in the graphene film and cracks where graphene either does not cover, or partially covers, the SiN_x membrane hole array. A typical Raman spectra obtained from the suspended graphene is shown in figure 2(c); it does not contain the D peak associated with defects and indicates high quality monolayer graphene.

Based on the non-contact optical method [2], the thermal conductivity κ of suspended CVD graphene membranes was measured by performing micro-Raman mapping of the selected area with different laser powers. A 532 nm wavelength laser beam was focused on the sample using a 100× objective lens with a numerical aperture of 0.9; the powers of the laser were set as 0.79, 2.1, 4.6 and 6.0 mW, respectively, and the pixel map was set as 150×150 over a 30 × 30 μm^2 map. During the mapping, the laser point moved pixel by pixel with a Raman spectra integration time (t) of 0.1 s. When the laser beam was focused on the suspended graphene on the Au/SiN_x substrate, the heat flux vector was along the radial direction away from the center of the graphene.

In order to estimate the time constant of (τ) of the transient heat transfer process, the Biot number (Bi) [12], was calculated by $Bi = gL_c/\kappa$, where g is the convective heat transfer coefficient and L_c is the critical dimension. Because L_c is relatively small and due to the high values of the measured κ [2], $Bi \ll 0.1$, which means that convection is the rate controlling process and dominates the time constant τ; therefore the lumped capacitance method could be used to estimate τ by [12]

$$\tau = \frac{\rho VC}{gA_s} \tag{1}$$

where ρ is the density of graphene, V is the volume of the sample, C is the thermal capacitance of graphene and A_s is the surface area of the graphene membrane in the suspended region. One finds that $\tau \ll 0.1$, so during the Raman spectral map acquisition the temperature has equilibrated.

The optical absorption through the center of the suspended graphene was measured using a semiconductor laser power meter (Newport, Model 1918-c) placed under the SiN_x support [3]. Due to randomly distributed wrinkles over the suspended graphene samples, the optical absorption was assumed to be the same for both wrinkle-free and wrinkled graphene samples. The obtained optical absorption was 2.9 ± 0.2% at 532 nm wavelength. The smaller error in the measured optical absorption compared to our earlier work [3, 4] is, we believe, due to improved transfer methods that leave less residue on the graphene. The measured optical absorption was used to determine the power (Q) transferred by the graphene. The temperature rise in the optically heated graphene causes a blue-shift of the Raman peak due to

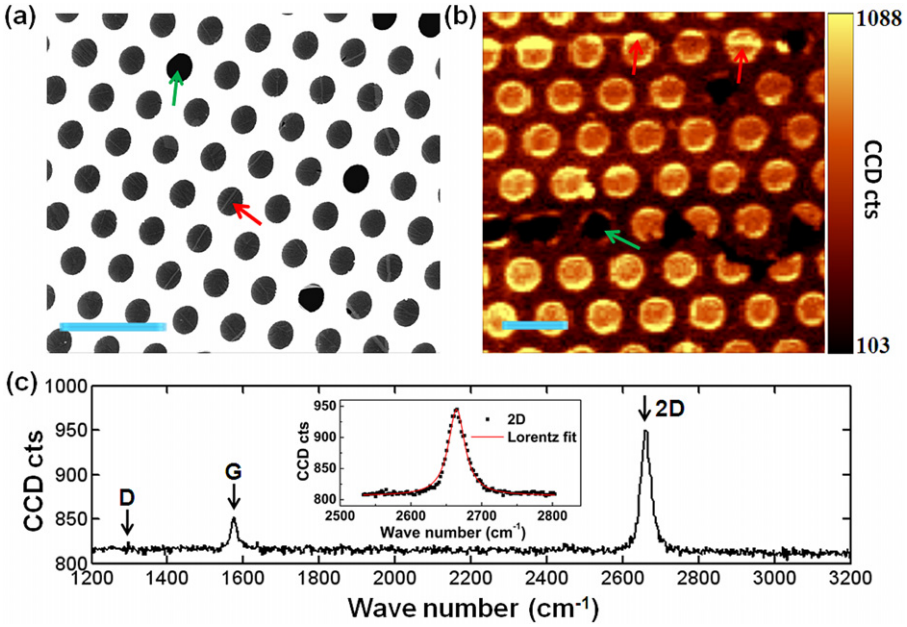

Figure 2. (a) SEM image and (b) Raman map (integrated intensity of the 2D peak (2630–2730 cm^{-1})) of graphene transferred onto the Au-coated SiN_x holey membrane. The red and green arrows in (a) and (b) indicate the wrinkles and cracks in some graphene samples. (c) Typical Raman spectrum of the wrinkle-free suspended graphene. The inset shows the Lorentz fitting of the Raman 2D peak.

increased anharmonic scattering of those optical phonons that are active in the Raman scattering processes. In this work, the rise in temperature of different graphene membranes was determined by the 2D peak shifts obtained from each suspended graphene membrane from the Raman maps. The 2D peak position was determined by a Lorentzian fit as shown in the inset of figure 2(c).

If one assumes that phonon transport is diffusive in the suspended region of the graphene monolayer and that the laser beam is focused on the center of each suspended graphene membrane, and ignores heat loss via radiation, the thermal conductivity κ of graphene is [3]

$$\kappa = \frac{\ln(\frac{R}{r_0})}{2\pi D R_g}\alpha \qquad (2)$$

where R is the radius of the holes; r_0 is the laser beam size of 0.17 μm [3], D is the thickness of the graphene, α is 0.98 for the 100× objective lens [3], R_g is the graphene thermal resistance given by $\frac{T_m - T_0}{Q - Q_{air}}$, T_0 is room temperature, T_m is the temperature rise determined by the shifts of the 2D peak obtained on the center of each suspended graphene membrane and Q_{air} is the heat loss in air as given by

$$Q_{air} = \int_{r_0}^{R} 2\pi g(T - T_0) r \, dr + \pi r_0^2 g(T_m - T_0) \qquad (3)$$

where the convective heat transfer coefficient g is 2.9 × 10^4 W m^{-2} K^{-1} [4].

3. Results and discussion

The micro-Raman mapping technique allows us to obtain statistics and study the variation between graphene membranes in one mapping. Twenty-six suspended wrinkle-free and crack-free graphene membranes were selected and the 26 obtained κ values at ~420 K are shown in the histogram in figure 3(a) and range from 1450 to 2350 W m^{-1} K^{-1}; this is close to a Gaussian distribution with an average value of 1875 W m^{-1} K^{-1}. The κ values obtained on 12 suspended wrinkled graphene membranes are also shown with a red histogram in figure 3 and are obviously lower, ranging from 1050 to 1950 W m^{-1} K^{-1} with an average value of 1482 W m^{-1} K^{-1}. Thus, the average κ value at 420 K measured on 26 suspended graphene membranes that were free of wrinkles was ~27% higher than the average value measured from 12 graphene membranes with wrinkles. The solid lines in figure 3, fitted by the Gaussian distribution, give an ~11% variance of κ for wrinkle-free graphene membranes and an ~20% variance for graphene membranes with wrinkles. Therefore, a significantly lower thermal conductivity with an increased experimental uncertainty was obtained for graphene membranes with wrinkles.

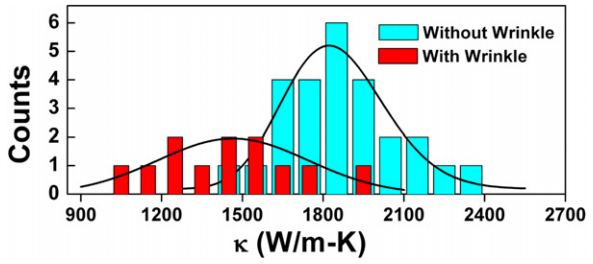

Figure 3. Histogram of the κ of 26 wrinkle-free graphene membranes and 12 wrinkled graphene membranes. The solid lines represent fits to the experimental data with the Gaussian distribution.

The error sources for the as-calculated κ are uncertainties of the temperature rise (T_m) determined by 2D peak shifts and

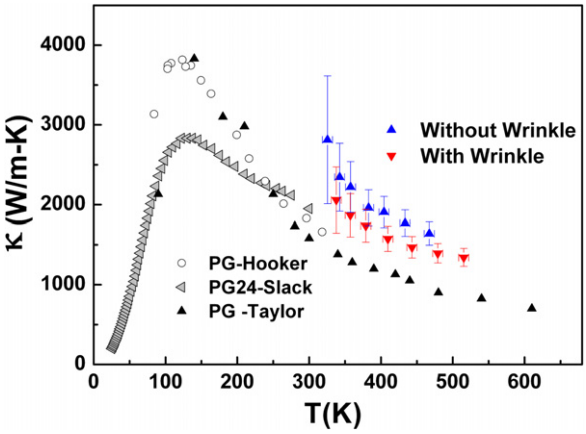

Figure 4. Typical thermal conductivities of the suspended graphene membranes with and without wrinkles as a function of the measured temperature of the graphene. Also shown for comparison are the literature thermal conductivity data of pyrolytic graphite samples as a function of temperature [13–15].

the measured laser absorption [3, 7]. Of these error sources, the uncertainty of 0.2% in the optical absorption with an average of 2.9% causes a ±7% variation in Q, which is by far dominant in its contribution to the uncertainty in the calculated value of κ.

Figure 4 plots typical results obtained for κ with increasing T_m, where the error in κ was calculated through the root-sum-square error propagation approach from the sources discussed above. The error sources considered are the Raman peak position temperature calibration, the temperature resolution of the Raman measurement method and the uncertainty of the measured laser absorption [4]. The trend of decreasing κ with increasing T_m for the graphene sample is attributed to increased phonon–phonon scattering with increased temperature. At near room temperature, the κ values of continuous graphene were as high as 2500 W m^{-1} K^{-1}. Higher κ was obtained for wrinkle-free graphene than for graphene with obvious wrinkles within the measured temperature range. It is worth noting that the difference between the thermal conductivity of wrinkled and unwrinkled graphene appears to be temperature-independent, which further supports the idea that the scattering mechanism responsible for the lower thermal conductivity value in wrinkled graphene is due to the existence of wrinkle/defects. The literature thermal conductivity data of pyrolytic graphite samples are also shown in figure 4 for comparison. The κ values obtained from the suspended wrinkle-free graphene and the graphene with obvious wrinkles were both higher than the reported in-plane values of pyrolytic graphite [13–15].

4. Conclusions

The thermal conductivity of graphene membranes was obtained by micro-Raman mapping. Thirty-eight membranes were measured with 26 being wrinkle free and 12 having wrinkles. An average value of κ of 1875 ± 220 W m^{-1} K^{-1} at 420 K was obtained for the wrinkle-free suspended graphene membranes, which is about 27% higher than the average value obtained from the wrinkled graphene membranes. Compared with results published recently (figure 1), and considering the apparent discrepancy in the optical absorption coefficient, the average thermal conductivity value for the wrinkle-free membranes studied here is consistent with the result from the Balandin group [2]. The relatively lower thermal conductivity obtained from wrinkled graphene membranes suggests that it is necessary to characterize the spatial distribution of the wrinkles, particularly in a large size graphene [6].

Acknowledgments

We appreciate support from the National Natural Science Foundation of China through grant Nos 91123009 and 10975115 and the Natural Science Foundation of Fujian Province of China (No. 2012J06002). The work at UT Austin was supported by the National Science Foundation Grant No. 1006350, the Office of Naval Research.

References

[1] Berber S, Kwon Y K and Tomanek D 2000 Unusually high thermal conductivity of carbon nanotubes *Phys. Rev. Lett.* **84** 4613–6
[2] Balandin A A *et al* 2008 Superior thermal conductivity of single-layer graphene *Nano Lett.* **8** 902–7
[3] Cai W W *et al* 2010 Thermal transport in suspended and supported monolayer graphene grown by chemical vapor deposition *Nano Lett.* **10** 1645–51
[4] Chen S S *et al* 2011 Raman measurements of thermal transport in suspended monolayer graphene of variable sizes in vacuum and gaseous environments *ACS Nano* **5** 321–8
[5] Chen S S *et al* 2012 Thermal conductivity of isotopically modified graphene *Nature Mater.* **11** 203–7
[6] Faugeras C *et al* 2010 Thermal conductivity of graphene in corbino membrane geometry *ACS Nano* **4** 1889–92
[7] Lee J U *et al* 2011 Thermal conductivity of suspended pristine graphene measured by Raman spectroscopy *Phys. Rev.* B **83** 081419
[8] Nair R R *et al* 2008 Fine structure constant defines visual transparency of graphene *Science* **320** 1308–8
[9] Li X S *et al* 2011 Large area graphene single crystals grown by low pressure chemical vapor deposition of methane on copper *J. Am. Chem. Soc.* **133** 2816–9
[10] Li X S *et al* 2009 Transfer of large-area graphene films for high-performance transparent conductive electrodes *Nano Lett.* **9** 4359–63
[11] Cai W W *et al* 2009 Large area few-layer graphene/graphite films as transparent thin conducting electrodes *Appl. Phys. Lett.* **95** 123115
[12] Incropera F P, DeWitt D P and Bergman T L 2007 *Fundamentals of Heat and Mass Transfer* 6th edn (New York: Wiley)
[13] Slack G A 1962 Anisotropic thermal conductivity of pyrolytic graphite *Phys. Rev.* **127** 694–701
[14] Taylor R 1966 The thermal conducivity of pyrolytic graphite *Phil. Mag.* **13** 157–66
[15] Hooker C N, Ubbelohde A R and Young D A 1965 Anistropy of thermal conductance in near-ideal graphene *Proc. R. Soc.* A **284** 17